Supporting Information: Photodynamics of Schiff Base Salicylideneaniline: Trajectory Surface-Hopping Simulations

Lasse Spörkel, Ganglong Cui,* and Walter Thiel*

Max-Planck-Institut für Kohlenforschung, Kaiser-Wilhelm-Platz 1, 45470 Mülheim an der Ruhr, Germany

E-mail: ganglong@mpi-muelheim.mpg.de; thiel@mpi-muelheim.mpg.de

Table of Contents

*To whom correspondence should be addressed

1 OM2/MRCI Active Space

The active space in the MRCI calculations included 12 electrons in 12 orbitals. Figure 1 shows the active orbitals for the most stable ground-state conformer of salicylideneaniline (cis-enol form).

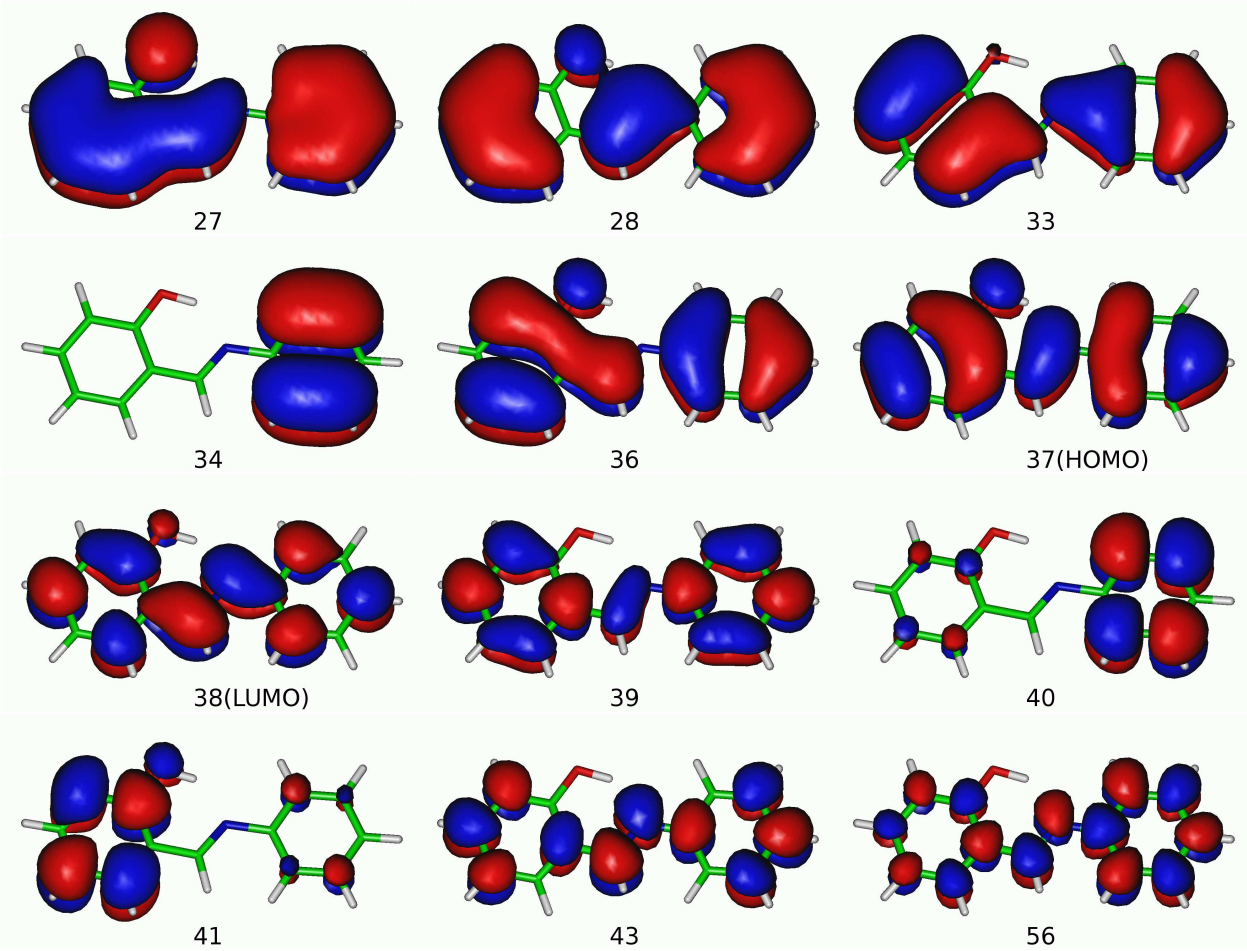

Figure 1: The active space (12e,12o) of salicylideneaniline (cis-enol form) used in the OM2/MRCI calculations. All orbitals are of π type. See text for simulation details.

In the closed-shell wavefunction of the planar ground state, the set of active orbitals consists of the 6 highest occupied π orbitals and the 6 lowest unoccupied π^* orbitals. During the simulations, an orbital tracking procedure[1] was applied to ensure that the active space remained intact also at non-planar geometries. Test calculations were done with an alternative choice of active orbitals, namely using the 6 highest occupied and 6 lowest unoccupied orbitals throughout (regardless of their character, selection solely based on energies). Static calculations with this alternative active

space gave results that are very similar to those reported here (data not shown), which is not too surprising since the most important orbitals are part of the active space in both cases.

2 Ground-State Potential Energy Profile

There are four relevant stable ground-state structures of salicylideneaniline (see Figure 2 of the main paper): the cis-enol form (S0-CIS-ENOL), the cis-keto form (S0-CIS-KETO), the trans-keto form (S0-TRA-KETO), and the twisted trans-enol form (S0-TRA-ENOL). S0-CIS-ENOL and S0-CIS-KETO can be interconverted by hydrogen transfer (via the transition state S0-TS-HT). The rearrangement between S0-CIS-KETO and S0-TRA-KETO requires rotation around the C8=C9 double bond (via S0-TS-KETO-ISOM). The geometries of these species have been optimized at the OM2/MRCI level (see Table 1 of the main paper) and at the B3LYP/6-31+G* level. The optimized Cartesian coordinates are given in sections 6 and 7 (see below). The relative energies are listed in Table 1.

Both at the OM2/MRCI and B3LYP/6-31+G* levels, the cis-enol form is the most stable structure followed by the cis-keto form (3–4 kcal/mol higher in energy). The two trans-conformers are less favorable, with energies of 11–13 kcal/mol (S0-TRA-ENOL) and 9–14 kcal/mol (S0-TRA-KETO) relative to the cis-enol form. The conversion of the cis-keto form to the cis-enol minimum is facile, with a barrier of 2–3 kcal/mol, while the trans-keto isomer has to surmount a large barrier of more than 30 kcal/mol to reach the region of the cis-keto isomer. The OM2/MRCI and B3LYP/6-31+G* relative energies agree well with each other (Table 1).

The OM2/MRCI nonadiabatic dynamics simulations show ultrafast $S_1 \rightarrow S_0$ internal conversion. After 1 ps three ground-state species are found (see section 5 below), namely the cis-enol, cis-keto, and trans-keto forms. In view of the computed ground-state barriers, any cis-keto species will quickly evolve towards the most stable cis-enol minimum, while the trans-keto form is expected to be trapped and to constitute the second photoproduct.

Table 1: Relative Energies (kcal/mol) of Ground-State Conformers and Transition States

Structure	OM2/MRCI	B3LYP/6-31+G*
S0-CIS-ENOL	0.0	0.0
S0-CIS-KETO	3.5	3.4
S0-TRA-KETO	9.4	13.8
S0-TRA-ENOL	12.7	11.0
S0-TS-HT	6.2	6.2
S0-TS-KETO-ISOM	51.9	43.9

3 Excited-State Reaction Coordinate

The path from the shallow S1-CIS-KETO excited-state minimum towards the conical intersection S1S0-CC-DB was traced by varying the dihedral angle N7-C8-C9-C14 in steps of 0.9° and performing constrained geometry optimizations at each point using OM2/MRCI. The resulting energy profile is shown in Figure 2. The energy rises by about 2 kcal/mol before it drops again after a rotation of about 50°.

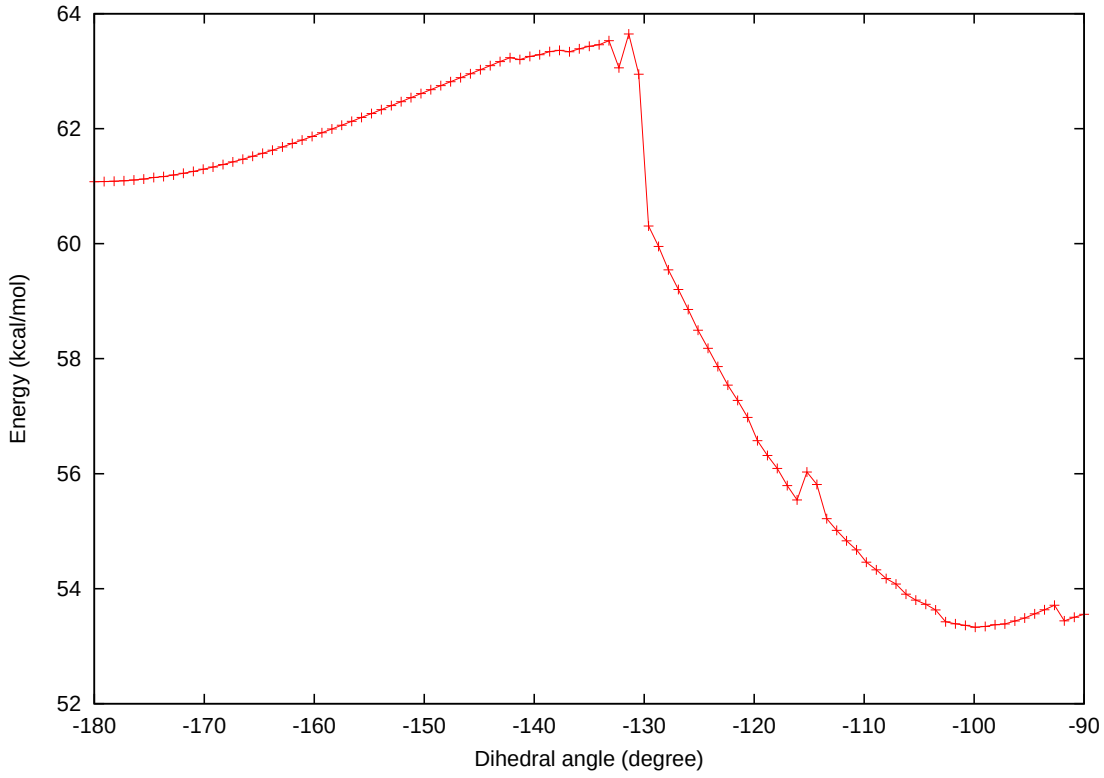

Figure 2: S_1 energy plotted against the dihedral angle N7-C8-C9-C10.

4 Vertical Excitation Energies

Theoretical and experimental $S_0 \rightarrow S_1$ vertical excitation energies of S0-CIS-ENOL and S0-CIS-KETO are presented in Table 2. The calculations were performed in the gas phase using OM2/MRCI and TDDFT (time-dependent density functional theory) at the corresponding ground-state geometries from OM2/MRCI and DFT(B3LYP), respectively (optimized coordinates see sections 6 and 7 below).

In the case of the cis-enol form, OM2/MRCI gives a vertical excitation energy of 3.91 eV. The TDDFT results are slightly lower (by 0.04–0.07 eV) for the M06-2X functional and the range-separated functionals (CAM-B3LYP, wB97X-D), and considerably more so for the B3LYP hybrid functional (by 0.40 eV). Also somewhat lower are the previously published TDDFT and CASPT2 values (3.63–3.75 eV) and the published experimental results obtained in solution (3.54–3.69 eV).

For the cis-keto form, the OM2/MRCI vertical excitation energy (2.90 eV) is slightly lower than the currently computed TDDFT values (2.95–3.18 eV). It lies in the range of the published TDDFT and CASPT2 values (2.79–3.26 eV), but above the experimental results in solution (2.60–2.62 eV). The first absorption of the cis-keto form is strongly red-shifted compared with the cis-enol form. OM2/MRCI predicts the corresponding shift in the vertical excitation energies to be 1.01 eV, which is close to the experimental data in solution (1.06–1.09 eV). This shift is underestimated by the current TDDFT calculations (0.56–0.69 eV) and by the published TDDFT and CASPT2 results (0.49–0.84 eV). Overall the OM2/MRCI performance appears to be quite satisfactory for the excitation energies.

5 Time Evolution of Key Geometric Parameters

Figure 3 illustrates the variation of the N7-C8-C9-C14 and C6-N7-C8-C9 dihedral angles during the simulations. The N7-C8-C9-C14 dihedral angle is indicative of cis and trans conformations at the C8-C9 bond. It starts out around 0° (cis-enol), reaches ca. 60° at the hopping points, and ends up in a very broad distribution covering both cis and trans conformers, with the latter being somewhat more frequent (see left side). The C6-N7-C8-C9 dihedral angle reflects the configuration around

Table 2: Theoretical and Experimental $S_0 \rightarrow S_1$ Vertical Excitation Energies (eV)

Reference	cis-enol	cis-keto
OM2/MRCI	3.91	2.90
TDDFT(B3LYP)/6-31+G*	3.51	2.95
TDDFT(CAM-B3LYP)/aug-cc-pVDZ	3.84	3.16
TDDFT(wB97XD)/aug-cc-pVDZ	3.87	3.18
TDDFT(M062X)/aug-cc-pVDZ	3.86	3.12
TDDFT(B3LYP)/6-31G* [Zgierski, 2000[2]]	3.75	3.26
TDDFT(B3LYP)/6-31+G** [Ortiz-Sánchez, 2008[3]]	3.66	2.82
CASPT2(10,10)/cc-pVDZ [Ortiz-Sánchez, 2008[3]]	3.63	2.79
Exp. (in methylcyclohexane) [Barbara, 1980[4]]	3.59	
Exp. (in acetonitrile) [Kownacki, 1994[5]]	3.69	2.60
Exp. (in acetonitrile) [Ziolek, 2004[6]]	3.68	2.62
Exp. (in acetonitrile) [Sliwa, 2010[7]]	3.54	

the N7=C8 double bond. It always remains around 180° during the whole simulation (see right side), thus clearly indicating that N7=C8 double bond isomerization does not play any role in the dynamics.

Figure 4 shows the distributions of the N7-H16 and O15-H16 distances in all trajectories. It is obvious from these plots that the $S_0 \rightarrow S_0$ internal conversion happens after the ultrafast excited-state proton transfer. At the starting geometries (top), the O15-H16 and N7-H16 distances cluster around 1.0 and 2.0 Å, respectively (cis-enol form with an O15-H16 covalent bond and an N7...H16 hydrogen bond). At the hopping points (middle), the H16 atom has in all trajectories been transferred to the N7 atom: the $S_1 \rightarrow S_0$ internal conversion thus occurs in the keto form that contains an N7-H16 bond (ca. 1.0 Å), with a broad distribution of O15-H16 distances that reflects the out-of-plane twist around the C8-C9 bond (see Figure 3). At the end points (bottom), three products can be identified: the cis-enol form with the H16 atom transferred back to the O15 atom as well as the cis-keto and trans-keto forms with an N7-H16 bond. Closer inspection of the bottom panel of Figure 4 shows that, after 1 ps, 32 of the 125 trajectories end up at an enol structure with an O15-H16 bond, while the remaining 93 trajectories are in the keto region with an N7-H16 bond. Among the latter, 69 have large O15-H16 distances of typically 4–5 Å (corresponding to the trans-keto form) and 24 have O15-H16 distances in the hydrogen bonding range around 2 Å (corresponding to the cis-keto

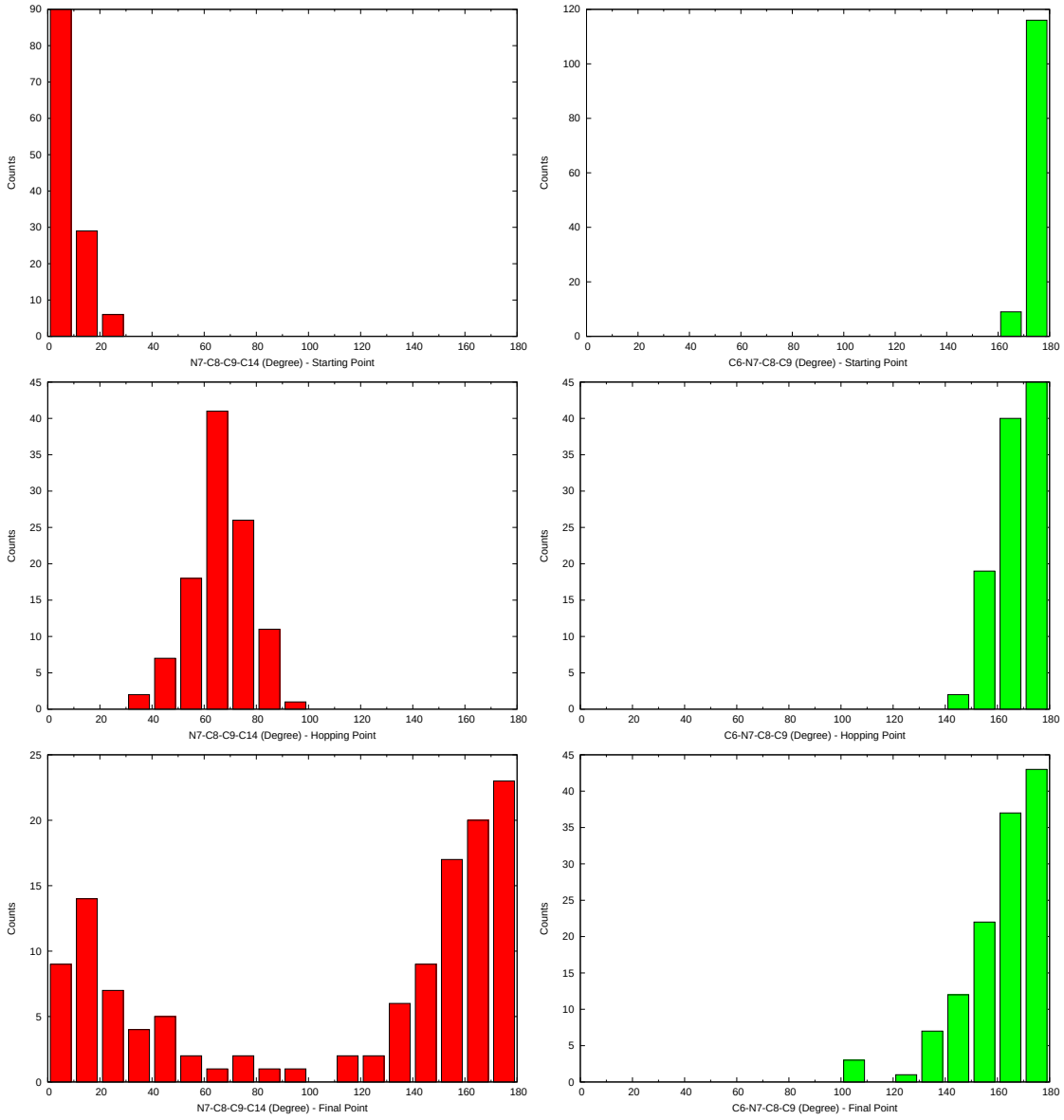

Figure 3: Distribution of key dihedral angles (degree) at the starting points (top), the hopping points (middle), and the end points (bottom).

form). Considering the ground-state energy barriers (see section 2 above), the cis-keto species will quickly rearrange to the most stable cis-enol minimum so that a total of 56 trajectories will yield the cis-enol photoproduct. The present simulations thus predict a branching ratio of 56:69 between the cis-enol and trans-keto photoproducts, i.e. about 45% vs. 55%.

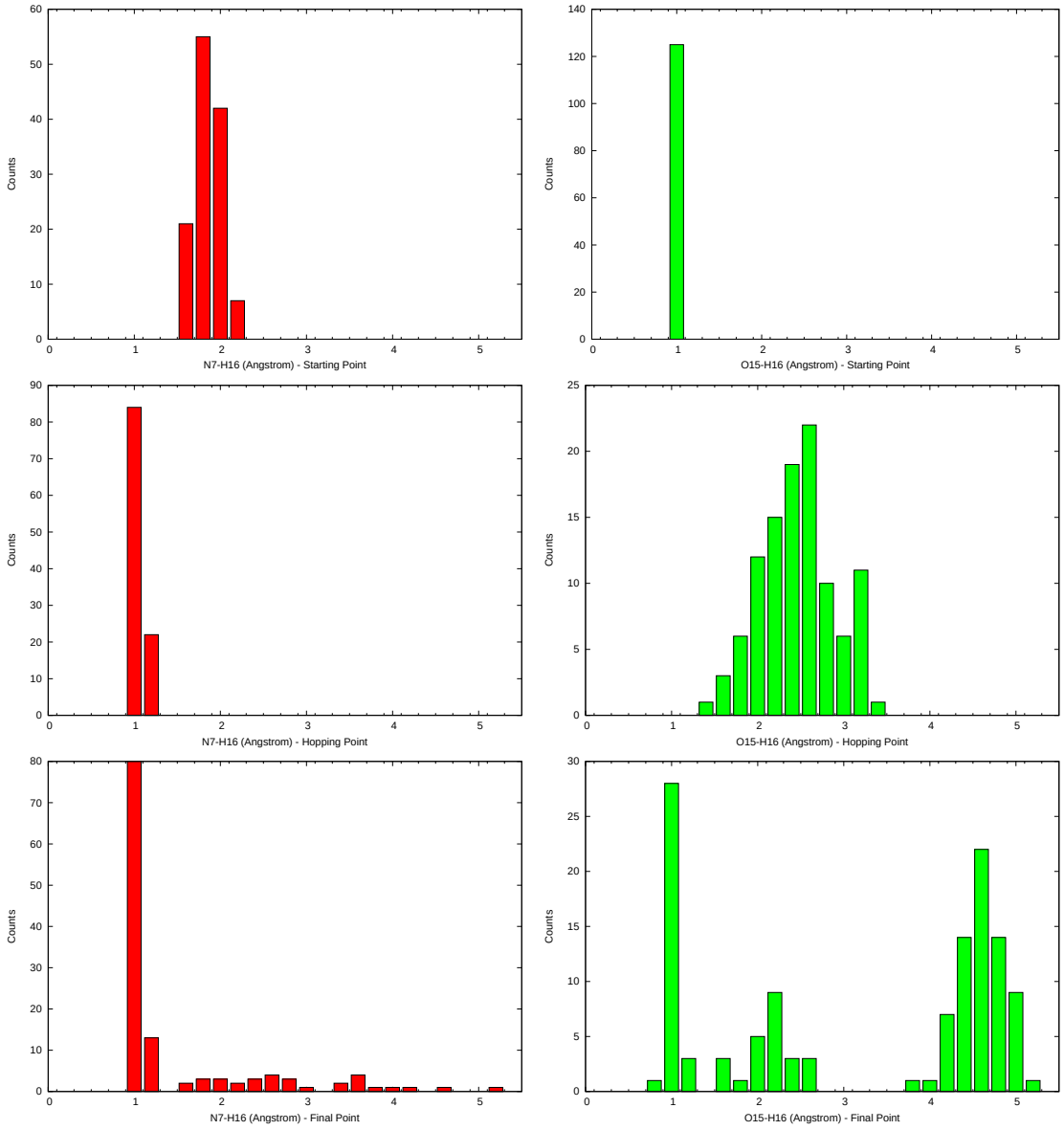

Figure 4: Distribution of key distances (Å) involving the mobile hydrogen for the starting points (top), the hopping points (middle) and the end points (bottom).

6 Cartesian Coordinates of All Optimized DFT Structures

S0-CIS-ENOL

C	0.14714	-3.05084	0.16272
C	-0.65487	-4.18342	0.17085
C	-2.05050	-4.03260	0.10855
C	-2.63109	-2.77051	0.03938
C	-1.82508	-1.62189	0.03105
C	-0.40845	-1.75510	0.09359
H	1.23012	-3.14974	0.20987
H	-0.20991	-5.17254	0.22457
H	-2.68943	-4.91221	0.11427
H	-3.70845	-2.64390	-0.00882
C	0.46806	-0.59936	0.08810
H	1.54165	-0.81919	0.13922
O	-2.42232	-0.41877	-0.03635
H	-1.70194	0.27383	-0.03117
C	0.84365	1.75358	0.01824
C	2.25140	1.74091	0.06078
C	0.18363	2.99317	-0.03813
C	2.96654	2.93753	0.04699
H	2.79900	0.80438	0.10368
C	0.90314	4.18801	-0.05134
H	-0.90223	2.99928	-0.07068
C	2.29961	4.16670	-0.00880
H	4.05293	2.91006	0.07963
H	0.37176	5.13516	-0.09513
H	2.86430	5.09506	-0.01933
N	0.01557	0.61099	0.02770

S0-TRA-ENOL

C	2.72323	-1.46479	-0.41091
C	4.06391	-1.12583	-0.52209
C	4.47915	0.16897	-0.17291
C	3.55815	1.10286	0.28841
C	2.20621	0.75687	0.40687
C	1.76308	-0.53738	0.04874
H	2.37289	-2.45583	-0.68175
H	4.78395	-1.85524	-0.88170
H	5.52605	0.44855	-0.25868
H	3.86046	2.10658	0.57135
C	0.35113	-0.91768	0.12801
H	-0.38122	-0.12406	0.35242
O	1.38528	1.74482	0.88342
H	0.48255	1.41882	1.01366
C	-1.44146	-2.39586	-0.05637
C	-2.39500	-1.55898	-0.66668
C	-1.86884	-3.59802	0.53479
C	-3.74777	-1.90576	-0.65207
H	-2.07061	-0.66157	-1.18722
C	-3.22267	-3.92882	0.56120
H	-1.12345	-4.25223	0.97801
C	-4.16944	-3.08479	-0.03117
H	-4.47218	-1.25721	-1.13884
H	-3.54008	-4.85410	1.03555
H	-5.22262	-3.35265	-0.02376
N	-0.06315	-2.11736	-0.05729

S0-CIS-KETO

C	0.14718	-3.10452	0.14824
C	-0.68125	-4.19571	0.14816
C	-2.09558	-3.99970	0.07544
C	-2.65326	-2.74832	0.00512
C	-1.83323	-1.55935	0.00088
C	-0.38000	-1.77534	0.07667
H	1.22748	-3.23344	0.20329
H	-0.27529	-5.20135	0.20273
H	-2.74523	-4.87284	0.07618
H	-3.72855	-2.60555	-0.04985
C	0.49525	-0.68470	0.07877
H	1.56681	-0.86192	0.13462
O	-2.33229	-0.39625	-0.06236
H	-0.96309	0.63300	-0.03515
C	0.84317	1.76017	0.00744
C	2.24538	1.76905	0.07190
C	0.14719	2.97766	-0.06878
C	2.93169	2.98371	0.05951
H	2.80884	0.84347	0.13156
C	0.84375	4.18464	-0.08043
H	-0.93875	2.96947	-0.11857
C	2.24026	4.19638	-0.01641
H	4.01733	2.97832	0.10986
H	0.29065	5.11809	-0.13983
H	2.78313	5.13716	-0.02546
N	0.07700	0.57998	0.01505

S0-TRA-KETO

C	0.33833	-2.53140	-1.25618
C	0.14325	-3.88139	-1.22245
C	0.04130	-4.55828	0.04463
C	0.13420	-3.88777	1.22762
C	0.34290	-2.44123	1.27765
C	0.44538	-1.76234	-0.04523
H	0.41315	-2.03569	-2.22394
H	0.06385	-4.45234	-2.14296
H	-0.11427	-5.63552	0.04674
H	0.05727	-4.39865	2.18316
C	0.64270	-0.39512	0.00045
H	0.70330	0.04732	0.98935
O	0.42844	-1.82470	2.35446
H	0.71165	0.03640	-1.97718
C	0.96872	1.83844	-1.02660
C	1.07063	2.57213	0.16501
C	1.06906	2.50418	-2.25856
C	1.27012	3.95210	0.11009
H	0.99694	2.08473	1.13091
C	1.26837	3.88321	-2.29956
H	0.99069	1.93971	-3.18599
C	1.37041	4.61764	-1.11496
H	1.34737	4.50888	1.04009
H	1.34367	4.38186	-3.26214
H	1.52570	5.69211	-1.14559
N	0.76704	0.44150	-1.04959

S0-TS-HT

C	0.12292	-3.11629	0.42271
C	-0.74251	-4.18851	0.35490
C	-2.10342	-3.95855	0.03035
C	-2.58926	-2.68885	-0.21902
C	-1.72455	-1.56093	-0.15848
C	-0.33476	-1.79812	0.16939
H	1.17232	-3.26906	0.67060
H	-0.39057	-5.19759	0.54699
H	-2.78378	-4.80580	-0.02281
H	-3.63272	-2.51684	-0.46575
C	0.53976	-0.67893	0.23948
H	1.58980	-0.82421	0.50363
O	-2.15152	-0.35117	-0.38324
H	-1.11489	0.37096	-0.22693
C	0.81987	1.71831	0.00057
C	2.20468	1.75065	-0.23467
C	0.12784	2.92141	0.21480
C	2.88451	2.96895	-0.22601
H	2.74609	0.83440	-0.45177
C	0.81519	4.13446	0.21882
H	-0.94460	2.89059	0.38666
C	2.19670	4.16470	0.00353
H	3.95491	2.98384	-0.41453
H	0.26925	5.05825	0.39090
H	2.73063	5.11093	0.00366
N	0.07235	0.52601	0.00564

S0-TS-KETO-ISOM

C	2.25879	-1.29099	0.59404
C	3.62931	-1.52667	0.50825
C	4.44463	-0.59185	-0.16980
C	3.93260	0.55878	-0.75096
C	2.52990	0.85062	-0.68058
C	1.73456	-0.14526	-0.01854
H	1.60889	-1.99184	1.11711
H	4.06304	-2.41652	0.95457
H	5.51554	-0.78015	-0.22994
H	4.58018	1.27383	-1.25288
C	0.34276	0.30705	0.00286
H	-0.09213	0.85533	0.84197
O	1.93544	1.89701	-1.12726
H	-0.03089	-0.35790	-1.80575
C	-1.81200	0.53830	-1.15277
C	-2.69453	0.56556	-0.06906
C	-2.21883	0.94777	-2.42564
C	-3.99420	1.03445	-0.26406
H	-2.38172	0.20646	0.90694
C	-3.52357	1.40715	-2.60941
H	-1.51413	0.93485	-3.25298
C	-4.41099	1.45529	-1.53070
H	-4.68504	1.05654	0.57383
H	-3.84122	1.73507	-3.59487
H	-5.42586	1.81374	-1.67697
N	-0.46667	0.07842	-0.99224

7 Cartesian Coordinates of All Optimized OM2/MRCI Structures

S0-CIS-ENOL

C	0.17783	-3.03188	0.05113
C	-0.66768	-4.13523	0.05781
C	-2.06278	-3.95924	0.05615
C	-2.62197	-2.68912	0.04787
C	-1.76481	-1.56334	0.04105
C	-0.35405	-1.72902	0.04265
H	1.26685	-3.16997	0.05243
H	-0.25011	-5.14586	0.06439
H	-2.71530	-4.84063	0.06150
H	-3.69883	-2.53071	0.04645
C	0.54455	-0.57369	0.03567
H	1.63768	-0.80974	0.03758
O	-2.37882	-0.37267	0.03326
H	-1.69603	0.36800	0.02882
C	0.85086	1.77336	0.02089
C	2.25423	1.76022	0.02150
C	0.16208	2.99860	0.01286
C	2.95361	2.96265	0.01414
H	2.80520	0.81283	0.02771
C	0.87599	4.19113	0.00557
H	-0.93145	2.99748	0.01246
C	2.26927	4.17604	0.00619
H	4.04960	2.95392	0.01461
H	0.34037	5.14676	-0.00069
H	2.82752	5.11807	0.00044
N	0.04479	0.61641	0.02792

S0-TRA-ENOL

C	0.12579	-2.94369	0.37200
C	-0.69918	-4.05383	0.47030
C	-2.06485	-3.95319	0.17933
C	-2.61071	-2.73532	-0.20279
C	-1.77717	-1.60252	-0.27940
C	-0.39585	-1.69219	0.00360
H	1.19565	-3.02722	0.60209
H	-0.28277	-5.02164	0.76876
H	-2.70155	-4.84132	0.24951
H	-3.66370	-2.63393	-0.46139
C	0.53793	-0.55386	-0.14588
H	1.45958	-0.82312	-0.70905
O	-2.37436	-0.48772	-0.76261
H	-1.98756	0.32617	-0.33793
C	-0.71048	1.03737	1.06384
C	-1.30566	0.23644	2.05581
C	-1.16377	2.35394	0.85715
C	-2.36193	0.75312	2.79872
H	-0.91367	-0.76009	2.26424
C	-2.23988	2.83714	1.59074
H	-0.66071	2.97819	0.11295
C	-2.84920	2.03386	2.55616
H	-2.81388	0.14724	3.59373
H	-2.61429	3.85251	1.41865
H	-3.70797	2.41652	3.11581
N	0.42287	0.63081	0.32037

S0-CIS-KETO

C	0.17637	-3.09544	0.14677
C	-0.67265	-4.17076	0.14554
C	-2.08606	-3.98021	0.07420
C	-2.63297	-2.73018	0.00543
C	-1.78413	-1.55684	0.00316
C	-0.34462	-1.76654	0.07643
H	1.26516	-3.23924	0.20164
H	-0.28258	-5.19129	0.19909
H	-2.72793	-4.87180	0.07605
H	-3.71015	-2.56853	-0.04948
C	0.52035	-0.66418	0.07745
H	1.61636	-0.83702	0.13379
O	-2.25654	-0.39453	-0.05924
H	-1.00090	0.67390	-0.03928
C	0.81430	1.76005	0.00601
C	2.22000	1.73670	0.07174
C	0.12459	2.98922	-0.06911
C	2.92166	2.94075	0.06174
H	2.76365	0.78828	0.13026
C	0.84794	4.17816	-0.07758
H	-0.96729	2.99707	-0.11980
C	2.24350	4.15896	-0.01247
H	4.01615	2.92743	0.11278
H	0.31724	5.13449	-0.13578
H	2.80514	5.09784	-0.01962
N	0.04216	0.58582	0.01171

S0-TRA-KETO

C	0.34658	-2.49349	-1.24652
C	0.15391	-3.84857	-1.20839
C	0.05844	-4.54098	0.04090
C	0.15560	-3.87816	1.22774
C	0.36060	-2.43751	1.25643
C	0.45604	-1.74468	-0.03223
H	0.41788	-1.97569	-2.21662
H	0.06933	-4.42737	-2.13346
H	-0.09626	-5.62808	0.01431
H	0.08501	-4.39071	2.18844
C	0.65203	-0.36763	0.03469
H	0.71769	0.07725	1.04309
O	0.45378	-1.80060	2.32041
H	0.69823	-0.00971	-1.97623
C	0.96025	1.81812	-1.03812
C	1.06499	2.53607	0.16901
C	1.05282	2.48883	-2.27620
C	1.26093	3.91526	0.12184
H	0.99455	2.02555	1.13279
C	1.24871	3.86722	-2.29584
H	0.97073	1.92605	-3.21183
C	1.35321	4.58358	-1.10090
H	1.34295	4.47769	1.05834
H	1.32096	4.39044	-3.25559
H	1.50704	5.66605	-1.12346
N	0.76222	0.42543	-1.05641

S0-TS-HT

C	0.15463	-3.12098	0.41084
C	-0.73664	-4.17184	0.34093
C	-2.10209	-3.93720	0.02802
C	-2.58427	-2.66773	-0.19481
C	-1.69012	-1.54818	-0.11916
C	-0.29855	-1.80001	0.16609
H	1.21287	-3.29440	0.64823
H	-0.40126	-5.19593	0.52559
H	-2.78038	-4.79940	-0.02252
H	-3.63219	-2.47315	-0.41922
C	0.58119	-0.67643	0.20655
H	1.66817	-0.84345	0.38012
O	-2.11149	-0.34567	-0.31932
H	-1.12372	0.44313	-0.18389
C	0.80537	1.71434	0.01547
C	2.19971	1.72698	-0.15238
C	0.09705	2.91775	0.17890
C	2.87154	2.94353	-0.16589
H	2.75185	0.79396	-0.30355
C	0.79224	4.12040	0.18510
H	-0.98643	2.89247	0.31637
C	2.17594	4.13751	0.01394
H	3.95106	2.96383	-0.34990
H	0.25144	5.05936	0.34252
H	2.71617	5.08930	0.01223
N	0.06147	0.51893	0.01282

S0-TS-KETO-ISOM

C	2.24882	-1.25080	0.60749
C	3.60785	-1.51051	0.49744
C	4.44169	-0.58420	-0.17280
C	3.92794	0.55639	-0.74068
C	2.52712	0.84863	-0.70856
C	1.69687	-0.10982	0.00044
H	1.60438	-1.96087	1.14719
H	4.04714	-2.40497	0.94106
H	5.52517	-0.77499	-0.19368
H	4.57941	1.27214	-1.24583
C	0.33307	0.35038	0.02351
H	-0.03611	1.04675	0.81760
O	1.98140	1.88880	-1.16853
H	-0.07046	-0.52116	-1.73452
C	-1.79669	0.54663	-1.15885
C	-2.68393	0.55284	-0.06846
C	-2.21039	0.96505	-2.43454
C	-3.98177	1.01536	-0.26782
H	-2.36420	0.18686	0.91077
C	-3.51866	1.40794	-2.60699
H	-1.50644	0.94821	-3.26993
C	-4.40035	1.44259	-1.52819
H	-4.67837	1.04019	0.57620
H	-3.84681	1.73330	-3.59785
H	-5.42146	1.81381	-1.67005
N	-0.45107	0.07095	-0.99138

S1-CIS-KETO

C	0.15616	-3.09345	0.14656
C	-0.74626	-4.21011	0.14296
C	-2.11142	-4.00396	0.07039
C	-2.63979	-2.70115	-0.00101
C	-1.77431	-1.56829	0.00025
C	-0.33157	-1.80999	0.07779
H	1.23539	-3.29191	0.20518
H	-0.33155	-5.22086	0.19858
H	-2.79454	-4.86133	0.06809
H	-3.71610	-2.53312	-0.05842
C	0.59608	-0.67300	0.08187
H	1.67789	-0.86062	0.14024
O	-2.21106	-0.37956	-0.06273
H	-0.96726	0.61689	-0.03855
C	0.82222	1.75152	0.00682
C	2.22921	1.76809	0.07350
C	0.10192	2.96417	-0.07056
C	2.89487	2.98634	0.06218
H	2.79359	0.83247	0.13362
C	0.79288	4.16704	-0.08012
H	-0.98998	2.94311	-0.12201
C	2.18597	4.18484	-0.01415
H	3.98988	3.00418	0.11390
H	0.23819	5.11020	-0.14004
H	2.72275	5.13819	-0.02225
N	0.08869	0.56516	0.01377

S1S0-CN-DB

C	1.77899	-2.20528	0.99616
C	1.81956	-3.29302	1.85342
C	0.70883	-3.66013	2.62611
C	-0.47577	-2.92301	2.54792
C	-0.52458	-1.83069	1.67276
C	0.59418	-1.42611	0.90297
H	2.65198	-1.91830	0.40048
H	2.74004	-3.88801	1.92888
H	0.75497	-4.54606	3.27108
H	-1.34639	-3.19445	3.13590
C	0.60700	-0.26443	0.06809
H	1.40114	-0.14719	-0.67585
O	-1.72756	-1.19105	1.64338
H	-1.76967	-0.58163	0.85921
C	-0.33064	1.67337	0.90323
C	0.82432	1.94107	1.69567
C	-1.44891	2.56165	0.97161
C	0.85080	3.05220	2.52100
H	1.67260	1.25486	1.65220
C	-1.39288	3.67519	1.79173
H	-2.33203	2.34224	0.36688
C	-0.25068	3.92168	2.56816
H	1.72587	3.25528	3.14451
H	-2.23985	4.36520	1.84081
H	-0.22058	4.80010	3.22424
N	-0.44570	0.62173	0.04395

S1S0-CC-DB

C	-0.13184	-2.82447	-0.65598
C	-0.98860	-3.92178	-0.72091
C	-2.14189	-3.99242	0.09265
C	-2.44225	-2.97358	0.96499
C	-1.58090	-1.81790	1.07628
C	-0.40220	-1.77776	0.22784
H	0.74438	-2.77149	-1.31072
H	-0.77624	-4.74623	-1.41098
H	-2.78394	-4.87804	0.02524
H	-3.33559	-3.00357	1.59013
C	0.52164	-0.65000	0.33168
H	1.23370	-0.63822	1.15533
O	-1.84437	-0.88622	1.86583
H	-0.59756	0.46616	-0.96114
C	0.90296	1.69675	-0.22987
C	2.15235	1.77789	0.41339
C	0.30369	2.84410	-0.79329
C	2.77747	3.01779	0.50050
H	2.63166	0.89022	0.84303
C	0.96008	4.06361	-0.69823
H	-0.66517	2.76695	-1.29642
C	2.19403	4.15981	-0.04933
H	3.74256	3.09269	1.00893
H	0.50252	4.96233	-1.12790
H	2.70170	5.14056	0.03833
N	0.23771	0.46539	-0.37937

References

(1) Keal, T. W.; Koslowski, A.; Thiel, W. *Theor. Chem. Acc.* **2007**, *118*, 837.

(2) Zgierski, M.; Grabowska, A. *J. Chem. Phys.* **2000**, *112*, 6329.

(3) Ortiz-Sánchez, J.; Gelabert, R.; Moreno, M.; Lluch, J. *J. Chem. Phys.* **2008**, *129*, 214308.

(4) Barbara, P.; Rentzepis, P.; Brus, L. *J. Am. Chem. Soc.* **1980**, *102*, 2786.

(5) Kownacki, K.; Mordzinski, A.; Wilbrandt, R.; Grabowska, A. *Chem. Phys. Lett.* **1994**, *227*, 270.

(6) Ziółek, M.; Kubicki, J.; Maciejewski, A.; Naskręcki, R.; Grabowska, A. *Phys. Chem. Chem. Phys.* **2004**, *6*, 4682.

(7) Sliwa, M.; Mouton, N.; Ruckebusch, C.; Poisson, L.; Idrissi, A.; Aloïse, S.; Potier, L.; Dubois, J.; Poizat, O.; Buntinx, G. *Photochem. Photobiol. Sci.* **2010**, *9*, 661.